Available online at www.sciencedirect.com
SCIENCE DIRECT®
International Journal of Mass Spectrometry 241 (2005) 89–97
International Journal of Mass Spectrometry
www.elsevier.com/locate/ijms

Aerosol particle mass spectrometry with low photon energy laser ionization

David G. Nash, X. Frank Liu, Erin R. Mysak, Tomas Baer*

Department of Chemistry, University of North Carolina, Chapel Hill, NC 27599-3290, USA

Received 29 October 2004; accepted 13 December 2004
Available online 7 January 2005

Abstract

The problem of excessive ion fragmentation observed in the mass spectra of organic aerosols is addressed by varying the photon energy used to ionize the vaporized particles. Oleic acid aerosols are vaporized by either an IR CO_2 laser or by impaction on a heater and ionized by pulsed laser radiation produced by either third harmonic generation in Xe (118 nm; 10.48 eV) or by resonance difference frequency mixing in Kr (142 nm; 8.75 eV). The use of the lower energy laser light greatly reduced the fragmentation of the oleic acid ions. However, spectra of oleic acid particles taken at several different CO_2 laser powers showed that the internal energy of molecules in the vapor plume vary in time so that the appearance of the mass spectrum is a function of the delay time between CO_2 and VUV laser pulses. Hot molecules produced in the early stages of vaporization generated large amounts of fragment ions, whereas the mass spectra of colder molecules consisted predominantly of parent ions. Vaporization with the heater on the other hand, shows a more uniform heating of the particle, with very little ion fragmentation. The ionization energy (8.6 ± 0.1 eV) and the fragment ion appearance energy (9.0 ± 0.1 eV) of oleic acid were determined by photoelectron photoion coincidence spectrometry.
© 2004 Elsevier B.V. All rights reserved.

Keywords: Oleic acid; RDFM; Laser; Heater

1. Introduction

Mass spectrometric analysis of aerosol particle constituents has become an essential tool not only for laboratory studies of model aerosols [1–8] but also in field studies, where rapid detection and identification of aerosols is highly desirable [9–16]. Atmospheric aerosols contain a wide range of substances including inorganic salts, metals, dust, soot, and organic species [17]. The ideal analysis tool should be able to identify each molecule, and provide a quantitative measure of its concentration. Unfortunately, current instruments are far from achieving this goal. This paper deals with the analysis of organic species in aerosol particles. The difficult issue in their analysis is the ease with which they fragment upon ionization. If a particle contains a large range of organic molecules, the identification is clearly impeded by extensive fragmentation, which results in a broad range of ion peaks whose identity is then difficult to establish.

Current aerosol mass spectrometers use either continuous or pulsed ionization schemes. The former generally employs electron impact [18,19], or chemical ionisation [20,21]. The pulsed ionization approach depends on lasers that are fired whenever a particle appears in the ionization region. This has the advantage that the laser photons are efficiently used when an aerosol particle is in the ionization region. The pulsed laser approach is ideal for large particles (0.2–5 μm in diameter) because their arrival at the ionization region can be determined by light scattering from continuous lasers [4,22,23]. The continuous ionization scheme is clearly advantageous for the detection of a large number of small particles whose arrival time cannot be detected by laser light scattering, and whose arrival at the ionization region is in any case quasi-continuous.

* Corresponding author. Tel.: +1 919 962 1580; fax: +1 919 843 6041.
E-mail address: baer@unc.edu (T. Baer).

1387-3806/$ – see front matter © 2004 Elsevier B.V. All rights reserved.
doi:10.1016/j.ijms.2004.12.016

Fragmentation of ions is a result of internal energy imparted to the ion during the vaporization or ionization process. Ionization by a pulsed UV laser, in which ionization is achieved by multiphoton excitation, results in particularly high ion internal energies because, once formed, the ion continues to absorb photons during the 5–10 ns photon pulse. It is not unusual to detect mostly C^+ ions and the observation of parent ion peaks is rare [8]. For this reason, a single laser ablation/ionization scheme does not work for organic species. In response to that, Worsnop and co-workers [19] have developed a two stage vaporization/ionization scheme in which the particles are directed at a heater located in the ionization region, where the vaporized molecules are ionized by electron impact. This provides excellent sensitivity and reduced fragmentation in comparison to the UV laser ablation/ionization scheme. However, ion fragmentation by electron impact of organic mixtures remains a difficult problem. Reducing the electron energy from 70 eV to lower energies would reduce fragmentation, but would also reduce the ionization efficiency.

Our approach to reducing ion fragmentation has been to use pulsed vacuum UV laser radiation [4], which has now also been implemented by Oektem et al. [24]. The aerosol particles are vaporized either by the absorption of infrared radiation from a pulsed CO_2 laser, or by impinging on a heater. Once vaporized, the molecules are ionized by 118 nm (10.48 eV) radiation generated by the frequency tripling of a 355 nm Nd:YAG laser pulse in a Xe/Ar mixture. This approach has dramatically reduced ion fragmentation because the 10.48 eV photon is close to the ionization energy of many molecules such as benzene, nitrobenzene, aniline, etc. However, we have found that as larger molecules with lower ionization energies are investigated, the 10.48 eV photon energy is too high and thus results in considerable ion fragmentation. This was a particular problem with the analysis of reaction products from the reaction between ozone and oleic acid aerosol particles [25]. The mass spectra of the reacted oleic acid particles vaporized by the CO_2 laser and ionized by the 10.48 eV VUV photons were characterized by a broad range of lower mass peaks that prevented identification of reaction products [25]. Thus, a softer ionization approach would be highly desirable.

As stated before, ion fragmentation is a result of high internal energy, which is caused both by heating of the neutral molecules with, for instance the CO_2 laser or the heating element, and by the VUV laser. Unfortunately, heating of the oleic acid cannot be avoided if sufficient material is to be vaporized for a strong ion signal. Thus the question arises; can we reduce ion fragmentation by reducing the energy of the VUV photon, or is the fragmentation an inevitable consequence of the vaporization process? For instance, Amirav [26] and Amirav and Danon [27] concluded that the fragmentation in electron impact could be dramatically reduced by cooling the sample in a molecular beam, thereby suggesting that the molecule's internal energy is a decisive factor in the fragmentation process. LaFranchi and co-workers have recently employed photoelectron resonance capture ionization (PERCI) to reduce fragmentation [28,29]. A similar reduction is possible with chemical ionisation [20,21]. In this paper, we address this issue by generating light at 8.75 eV, which is nearly 2 eV lower than the previously used 10.48 eV. The nature of the vaporization method of oleic acid particles is also explored to better understand how different vaporization conditions affect the oleic acid mass spectrum.

2. Experimental approach

The current experimental set-up can be seen in Fig. 1. The oleic acid particles in this study were generated by atomizing a 1:10 oleic acid:isopropanol mixture with a glass nebulizer (Meinhard). The particles were then sent into an aerodynamic lens as described by Liu et al. [30,31], where they were focused and accelerated by gas expansion into the vacuum. The particle velocity, and thus their size, was determined by detecting scattered light as they passed through two green, continuous laser beams. The scattered light signals were sent into a timing circuit, which triggered the CO_2 laser to fire as the particle reached the TOF extraction region. After a variable delay between 2 and 20 μs, the vapor plume was ionized via VUV irradiation ($\lambda = 142$ nm).

The VUV radiation was generated by resonance difference frequency mixing (RDFM) as shown in Fig. 2 [32]. The 355 nm output from a Nd:YAG laser (Continuum) pumped a dye laser (Continuum) with an Exalite 428 dye to produce 425 nm light. This light was doubled with a BBO crystal in an Inrad Autotracker III, yielding $\lambda = 212.5$ nm light. The $\lambda = 425$ nm (2 mJ) and 212.5 nm (10 mJ) pulses were steered through a series of prisms, and directed into a Kr cell ($P_{Kr} = 10$ Torr) where RDFM produces the desired 142 nm (8.75 eV) light. The exit of the mixing cell was terminated by a LiF lens with a focal length of 20 cm, which causes the 142 nm light to slightly converge, leaves the 212 nm light nearly parallel, and the 425 nm light slightly divergent. This arrangement minimized the absorption of the 212.5 and

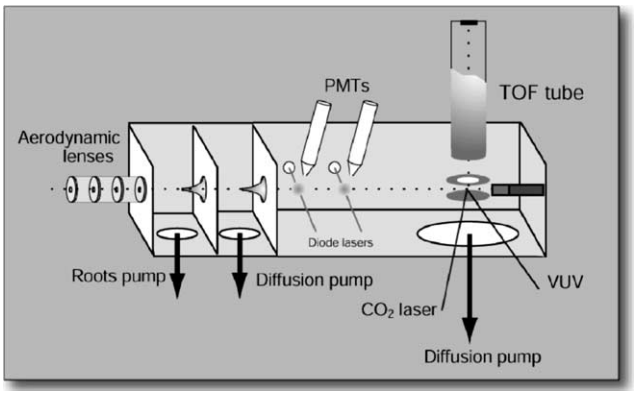

Fig. 1. Schematic of single aerosol particle laser TOF instrument. Particles are focused in the aerodynamic lens, detected and sized in the two light scattering regions, then vaporized and ionized in the extraction region of the TOF-MS.

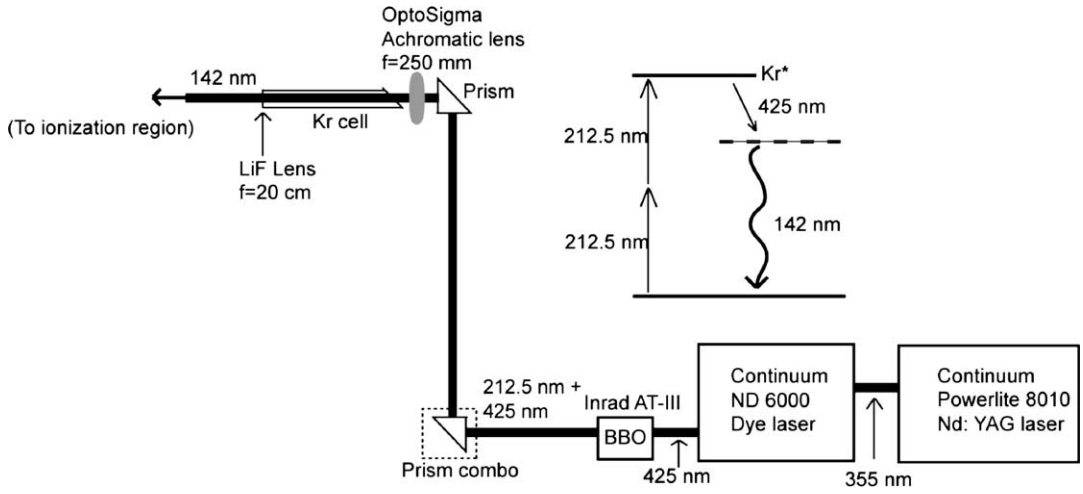

Fig. 2. Schematic of resonance difference frequency mixing (RDFM) set-up. Both $\lambda = 425$ and 212.5 nm enter the Kr mixing cell, and the resultant 142 nm light is then focused into the main chamber via a LiF lens.

425 nm light by the ion. Future experiments will pass the output through a LiF wedge prism to completely eliminate the lower energy photons from the ionization region.

The ions generated by the VUV light were accelerated out of the ionization region by a DC extraction field and into the flight tube after which they were detected by a pair of multichannel plates (MCPs). Each firing of the CO_2 and VUV lasers produced a complete single particle mass spectrum on a digital oscilloscope (HP, Infinium), which digitized each mass spectrum and transferred it to a PC through a GPIB connection. Though the particles produced with the nebulizer were polydisperse, the timing circuit that controls the firing of the CO_2 and VUV (or just the VUV in the case of heater vaporization) lasers was adjusted to only trigger on 3–4 μm particles. The total count rate of particles of all sizes was sufficiently low (ca. 20 per second) that the uncounted particles were pumped away long before the size selected particles were analyzed so that they did not interfere with the analysis. Typically, a mass spectrum was recorded by averaging 100 single particle mass spectra.

A threshold photoelectron photoionization coincidence (TPEPICO) study of oleic acid was undertaken in order to examine the ionization energy of oleic acid and the onset energies of its fragment species. Ions are energy selected by TPEPICO, which collects mass spectra of ions in coincidence with their zero-energy electrons, yielding information on fractional abundance of parent and daughter ions as a function of the photon energy. The apparatus has been described in detail elsewhere [33,34]. Briefly, a gaseous sample was directly introduced into the ionization region of the mass spectrometer. Because of the low vapor pressure of oleic acid at room temperature, it was necessary to introduce the sample with a heated inlet of approximately 430 K as monitored by a thermocouple. The oleic acid sample was ionized with VUV light from a H_2 discharge lamp, dispersed by a 1m normal incidence monochromator. Electrons and ions were continuously extracted in opposite directions by a 20 V/cm field. The electron signal collected by a channeltron electron multiplier served as the start time for ion time-of-flight (TOF) collection, and the ion signal collected with a multichannel plate detector served as the stop time for the ion. Each coincidence event was stored on a multichannel pulse height analyzer. Low sample signal made it necessary to collect spectra for periods on the order of hours at each wavelength.

3. Results and discussion

Fig. 3 shows a comparison of an oleic acid mass spectrum taken with 118 nm light and one taken using the RDFM wavelength of 142 nm (8.75 eV). The amplitude of the $m/z = 282$ peak is approximately eight times higher for the spectrum obtained via RDFM than for the 118 nm case. This is partly a

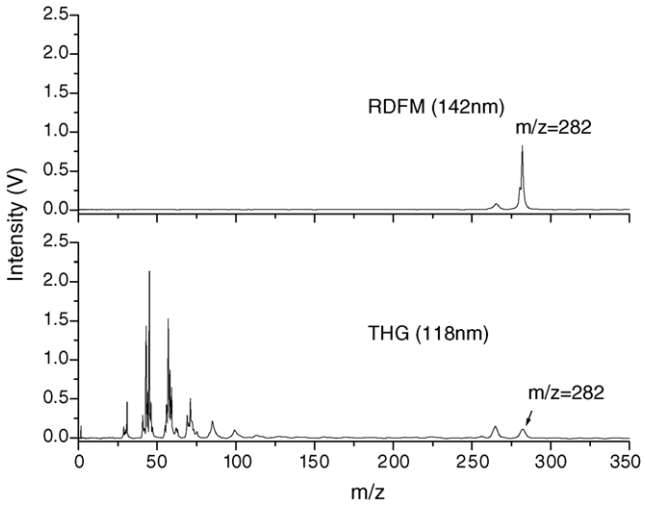

Fig. 3. Oleic acid spectra obtained with a CO_2 laser power of 70 mJ/pulse and VUV wavelengths of (a) 142 nm and (b) 118 nm. The vertical axis is the ion signal measured as a voltage on the oscilloscope.

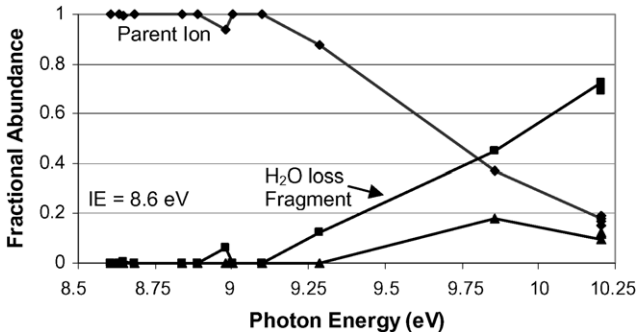

Fig. 4. The fractional abundance of parent and two fragment ions for energy selected oleic acid ions prepared by threshold photoelectron photoion coincidence (TPEPICO).

result of the reduced fragmentation in the RDFM case. With the 142 nm light, the only fragment observed is due to water loss, yielding a peak at $m/z = 264$. Reduced fragmentation not only allows for easier identification of $m/z = 282$, but the absence of other fragments greatly facilitates the analysis of mixtures.

No literature value for the ionization energy of oleic acid exists. However, the strong mass spectral signal observed with 8.75 eV laser ionization indicates that its IE is less than this.

Photoionization at various wavelengths was used to determine that the ionization energy of oleic acid is 8.6 ± 0.1 eV. The breakdown diagram of oleic acid in Fig. 4 shows fractional abundances of the molecular ion, $m/z = 282$, and two daughter ions, $m/z = 264$ and 256 as a function of VUV photon energy. In order to obtain the ion energy from the photon energy, it is necessary to add to the photon energy the ion internal energy, which depends on the temperature of the experiment (430 K, in this case). If the temperature of the CO_2 laser vaporized aerosol particle were similar to the temperature of the TPEPICO experiment, the 8.75 eV VUV photon ionization should yield only the parent ion. The fact that we observe a water loss peak indicates that the laser vaporized molecules have a higher internal temperature than the gas phase oleic acid molecules vaporized at 430 K.

The onset for water loss signal in the breakdown diagram of Fig. 4 appears at about 9.1 eV. However, the ion TOF distributions indicate that at this energy, the parent ion is metastable and loses water slowly. The true thermochemical dissociation limit may lie well below 9.1 eV, but no fragment ions are observed because the low dissociation rate constant does not permit the ion to dissociate on the timescale of the ion TOF collection, which is on the order of 20 μs. This effect causes the fragment appearance energy of 9.1 eV to be higher than its true thermochemical dissociation energy. On the other hand, the ions initially contain considerable thermal energy as a result of heating the sample to 430 K. This causes the appearance energy (observed onset) of the water loss peak to be shifted toward lower energy. Without a detailed analysis that takes calculated dissociation rate constants and the thermal energy distribution into account, it is indeed difficult to determine a precise dissociation energy for the water loss peak. An approximate dissociation energy is 9 eV.

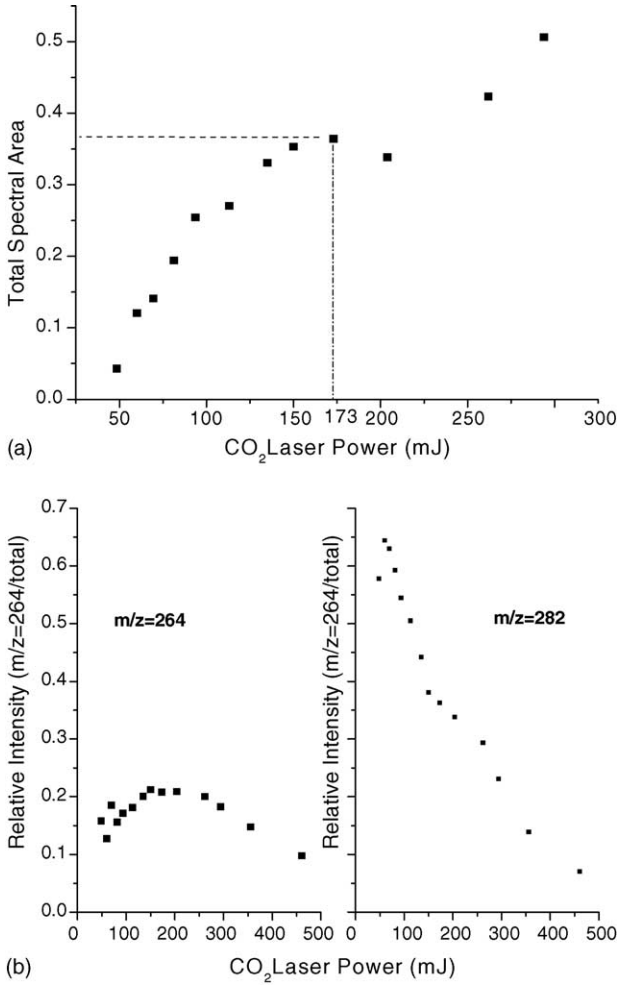

Fig. 5. (a) Total mass spectral intensity as a function of CO_2 laser power for oleic acid. The dashed vertical line represents the threshold power for complete particle vaporization. (b) Plot of $m/z = 264$ and 282 relative intensities with respect to CO_2 power.

3.1. The effect of CO_2 laser power and VUV laser delay

Fig. 5 relates the CO_2 laser power to the total mass spectral signal. Initially, the total oleic acid spectral area increases with increasing CO_2 laser power as more of the particle is vaporized. At a CO_2 power of approximately 173 mJ/pulse, the total oleic acid signal begins to plateau, an effect similar to that seen by Woods et al. in their study of *m*-nitrotoluene particles [3]. This leveling of the spectral area is an indication that laser heating results in complete vaporization. For this experiment, the delay between the application of the CO_2 and VUV laser pulses was adjusted to achieve optimal signal intensity. This was necessary because the translational energy of the vaporized molecules increases with the CO_2 laser power, thus necessitating the reduction of the delay between the two lasers.

As shown in Fig. 5, the maximum relative intensity for the oleic acid parent peak ($m/z = 282$) is located at ~75 mJ/pulse. The maximum of the $m/z = 264$ intensity, which occurs at ~173 mJ/pulse is coincident with the location of the threshold power. This suggests that up to 173 mJ/pulse, the CO_2 laser puts only enough excess internal energy into the vaporized oleic acid molecules to produce $m/z = 264$ when the molecule is ionized with VUV irradiation. At powers greater than 173 mJ/pulse, both the parent peak and the $m/z = 264$ peak decrease with increasing CO_2 laser power. After ~200 mJ/pulse, however, the total oleic acid mass spectral area begins to increase, possibly as a result of the dissociation of neutral oleic acid into two fragments, both of which can be ionized by the VUV laser. At lower CO_2 laser powers where the oleic acid ion primarily loses just water, only the $m/z = 264$ fragment can be ionized by the 8.75 eV VUV laser, while the water fragment cannot.

One of the interesting questions deals with the mechanism for fragment ion production. Two scenarios could account for their observation:

$$\text{Oleic acid} \xrightarrow{h\nu(CO_2)} \text{neutral fragments} \xrightarrow{h\nu(\text{VUV})} \text{fragment ions} \quad (1)$$

$$\text{Oleic acid} \xrightarrow{h\nu(CO_2)} (\text{oleic acid})^* \xrightarrow{h\nu(\text{VUV})} \text{fragment ions} \quad (2)$$

In the first case, the CO_2 laser dissociates the oleic acid into neutral fragments, which are then ionized by the VUV laser. In the second mechanism, the CO_2 laser just heats up the oleic acid, and the fragment ions are produced by dissociative ionization. In general, the second mechanism is more likely because ionic species have lower dissociation energies than neutral species. But, given sufficient CO_2 laser power, it is possible that both mechanisms pertain here. The increase in the total ion signal after about 200 mJ of CO_2 laser power seen in Fig. 5 can be accounted for by mechanism (1) because the dissociation of the neutral oleic acid generates two fragments that are candidates for ionization by the VUV laser, whereas, mechanism (2) will only generate one ion.

In an effort to distinguish the effects of mechanisms (1) and (2), the CO_2–VUV delay time was varied for several different CO_2 laser powers. At each laser power, as the delay time increased, the ratio of the ($m/z = 282$)/($m/z = 264$) peak areas also increased. The effect is even more dramatic at 294 mJ IR laser power. At long delay times, the lower mass fragments are nearly absent, whereas they are dominant at 4 μs delay time. The interpretation of the changing mass spectra as a function of the VUV laser delay depends on whether mechanism (1) or (2) is operative. Suppose that mechanism (1) is dominant so that the observed fragment peaks in Fig. 6 originate from the ionization of neutral fragments. If particles were heated and vaporized homogeneously, all molecules (fragments and parent molecules) would have the same temperature and thus the same translational energy distribution. But, the neutral fragments would have a higher velocity as a result of their lower mass. The VUV laser has a focal region of about 3 mm^2. The center of the VUV laser spot is offset from the center of the CO_2 by ~1 mm, and the aerosol particle, therefore, requires some time to expand to fill the VUV spot after vaporization. Fast fragments might, therefore, arrive before the heavier parent molecules. However, calculated Maxwell–Boltzmann distributions of molecular velocities for each ion species at several different temperatures show that the difference in the velocity between the $m/z = 264$ fragment and the $m/z = 282$ parent is so small that it cannot account for the large change in the ion intensities at for instance 294 mJ (Fig. 6). Nor can the large intensity of the smaller fragments at short times be accounted for in this manner.

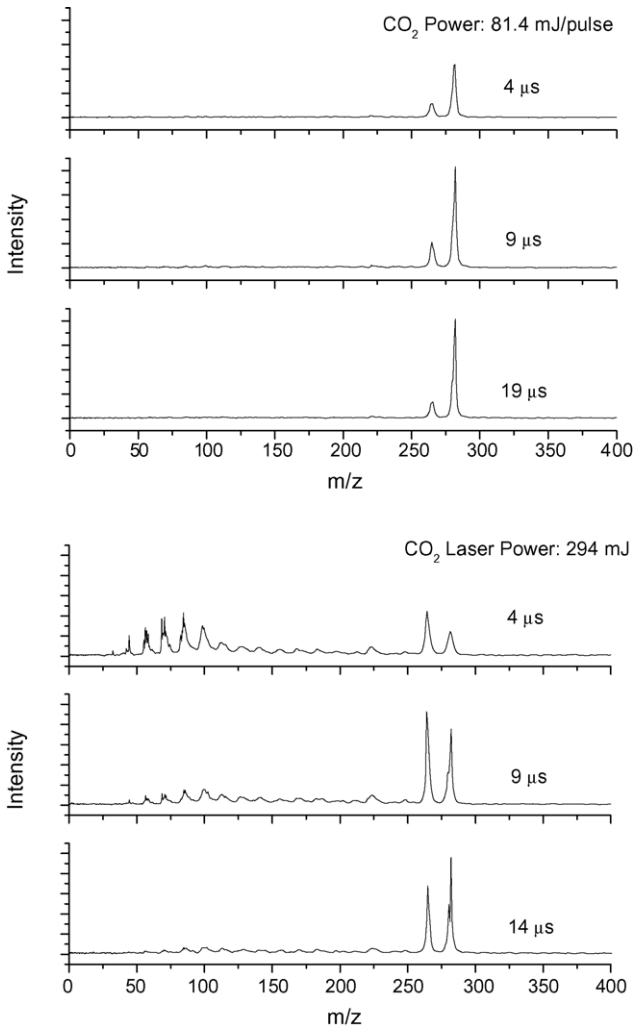

Fig. 6. Oleic acid spectra at various CO_2 powers and CO_2–VUV delay times. The vertical axes are the same for each spectrum within the given CO_2 power. The $m/z = 282$ signal is ~0.5 V for the 14 μs delay at 294 mJ, and ~0.8 V for the 19 μs delay at 81.4 mJ.

The second mechanism, in which the CO_2 laser simply heats the oleic acid and the fragment ions are generated by dissociative ionization, is also not consistent with a single temperature for the sample. In this mechanism, all mass spectra should have the same mass peaks in the same relative pro-

portions independent of the VUV laser delay time because the ion precursor is always the parent molecule.

Because of this non-uniform temperature, we cannot distinguish mechanisms (1) and (2) on the basis of the data in Fig. 6. The only evidence for mechanism (1) is the increased ion signal as observed in Fig. 5a.

Two sources of non-uniform temperatures can be postulated. It is possible that the laser does not heat the particle uniformly so that parts of the particle are hotter than others. As pointed out by Woods et al. [3], the time required for the thermal equilibration of a 2 μm particle is on the order of 10 μs. This is longer than the time required to vaporize the particle, so that the non-uniform distribution of temperatures could be transferred to the vapor phase. The hot parts of the particle would eject their vapor more rapidly thus accounting for the change in the mass spectra with IR–VUV laser delay times. It is also possible that even if the particle is initially heated uniformly, the vaporization process itself can cool the particle during the course of evaporation. That is, while "hot" molecules are ejected from the surface of the particle, the expansion of the particle itself can lead to cooling of interior molecules, thereby generating a temperature gradient during the course of evaporation.

Molecules and/or fragments detected at a delay time of 14 μs were calculated to have a temperature of ∼57 K, while those detected at a delay of 4 μs had a calculated temperature of ∼700 K. Therefore, species detected at shorter delay times are "hotter" and possess more vibrational energy than the "colder" species detected at longer delays, thereby accounting for the degree of fragmentation as a function of delay time, and thus the changing (m/z = 282)/(m/z = 264) ratio. It is likely that mechanism (1) is dominant at high CO_2 laser powers.

3.2. Use of heater with VUV laser

In a previous study [35], we showed that aerosol particles can also be vaporized by letting them impinge on a heater, as is done in the instrument of Jayne et al. [19]. In our case, oleic acid particles fly through the ionization region, hit the heater and are vaporized, and travel back to the ionization region before being ionized by the VUV laser. So, for a particle with an incoming velocity of 100 m/s before vaporization, and a resultant vapor molecule velocity of 220 m/s (at a 640 K heater temperature), it takes a particle on the order of 60 μs to arrive at the heater after first crossing through the extraction region, and on the order of 30 μs for resulting vapor molecules to return to the extraction region for ionization. Fig. 7 shows an example of an oleic acid particle mass spectrum taken using the heater for particle vaporization.

Contrary to vaporization using a CO_2 laser, use of a cartridge heater provides homogeneous heating of oleic acid particles. As mentioned, the mean velocity of m/z = 264 and 282 molecules are very similar at a given temperature. Therefore, if particles are indeed heated homogeneously, a constant ratio of (m/z = 264)/(m/z = 282) should be expected independent of VUV delay, as indeed observed experimentally in Fig. 8.

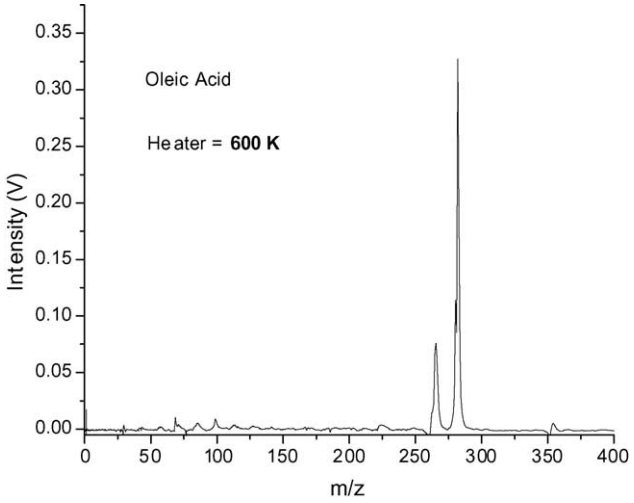

Fig. 7. Oleic acid particle mass spectrum taken with the cartridge heater at 600 K. Background signal has been subtracted.

Given that the heater provides homogeneous particle heating, calculation of the average energy of oleic acid ions as a function of temperature was performed to try to understand the fragmentation pattern upon ionization at the vaporization temperatures used in this experiment (Fig. 9). These average energy calculations indicate that at 700 K, oleic acid has an internal energy of approximately 2.7 eV. When these molecules are ionized by an 8.75 eV photon, the ion can be generated in a range of energies from the ionization energy of 8.6–11.45 eV. According to the breakdown curve in Fig. 4, this should result in substantial fragmentation of the ions. But the observation of fragment ions depends upon the time scale of the experiment because of the low dissociation rate constants. The breakdown diagram in Fig. 4 was taken with

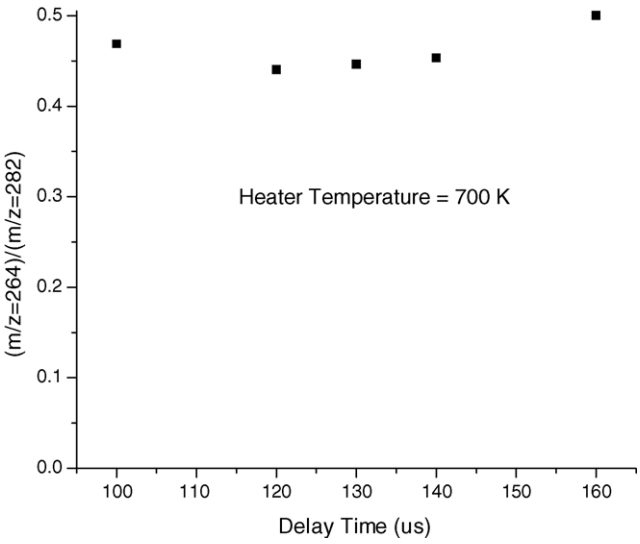

Fig. 8. The (m/z = 264)/(m/z = 282) ratio as a function of VUV delay time using a cartridge heater at 700 K for the vaporization step.

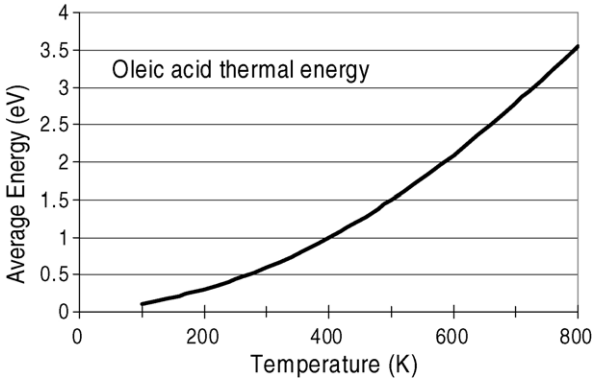

Fig. 9. Calculated average oleic acid internal energy as a function of temperature using the calculated oleic acid vibrational frequencies.

a 20 V/cm extraction field and the ions were accelerated over a 5 cm region, whereas in the aerosol experiment, the extraction field was 200 V/cm and the extraction distance was just 1 cm. Thus, the time to extract an ion of mass 282 is 12.1 μs in the TPEPICO case and 1.7 μs in the aerosol instrument. That is, the ions have a residence time of 7.1 times longer in the TPEPICO instrument than in the aerosol instrument. By delaying the extraction pulse in the aerosol instrument, we can lengthen this residence time and thus increase the fragment ion signal. This is verified in Fig. 10 where the ratio of parent to daughter ion signal changes from 1.72 to 1.27 as the delay time is increased from 0 to 3 μs. That is, the longer we wait before extracting the ions, the more time is provided for the ion to dissociate. These data were corrected for a background signal discussed in the following section.

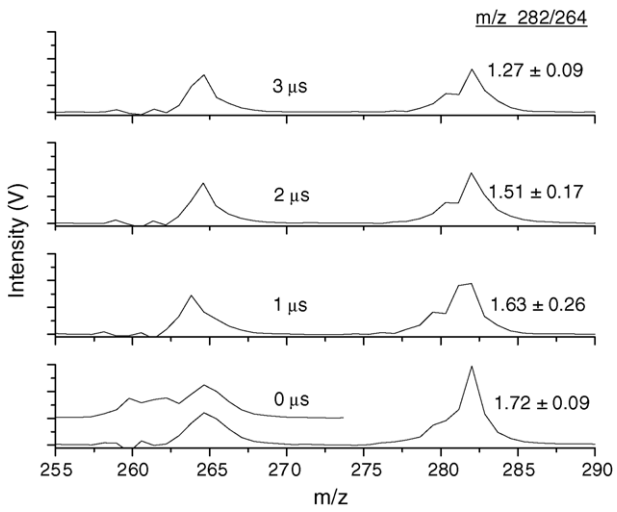

Fig. 10. The mass spectra of oleic acid particles at a heater temperature of 700 K at the pulsed extraction delay times. The ratio of (m/z = 282)/(m/z = 264) peak areas is shown on the right for each delay time. The variation of this ratio with pulsed extraction delay is a reflection of the slow dissociation of the parent oleic acid ion. Background signals (Fig. 11) have been subtracted from the spectra. For comparison, the raw particle spectrum before background subtraction for 0 μs delay is vertically offset from the background subtracted spectrum. Additionally, it should be noted that the vertical axis for each of the spectra are the same.

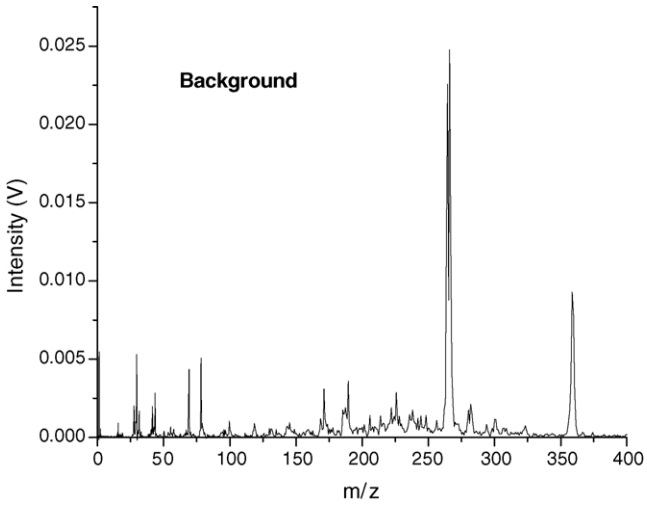

Fig. 11. Background signal without particles. Obtained using only the VUV laser.

3.3. Comparison of particle evaporation by heater and CO_2 laser

Overall, the heater is preferential to the CO_2 laser because it heats particles homogeneously, and as such, yields similar parent/fragment ratios across a range of VUV delay times. One drawback with the heater is that the overall intensity is lower because the heater tip can only be placed within approximately 6 mm from the center of the extraction region. Calculations show that this distance from the extraction region should cause signal obtained with heater vaporization to be ∼2.8 times lower than signal obtained using the CO_2 laser. These calculations involved determining the percentage of the vapor plume that would be contained within the VUV laser spot area for each vaporization method. Comparison of the signal level for an oleic acid mass spectrum collected with a CO_2 power of 81.4 mJ with a mass spectrum collected with a heater temperature of 640 K showed a CO_2 signal/heater signal ratio of ∼3.2, which is close to the predicted ratio of 2.8.

An interesting feature common in all spectra taken in this study is the background signal (Fig. 11). This spectrum was obtained by firing the laser at a time when no particle is passing through the ionization region. It is evident that this spectrum looks completely different from the particle mass spectrum in that the oleic acid peak at 282 is barely visible. On the other hand, a new peak appears (actually a doublet at m/z = 258 and 261) which does not line up with the water loss peak at 264. The origin of this background was determined to be a result of the residual 212 nm light that is co-propagating with the VUV light. Because the peaks do not line up with the water loss peak, it was rather easy to subtract its contribution from the data in Fig. 10. Efforts are currently underway to solve this problem by introducing a LiF wedge prism into the experimental set-up, which will separate the 212 nm light from the 142 nm light, preventing the 212 nm light from entering the ionization chamber.

The set-up used in this study shows great promise for the study of heterogeneous gas-particle reactions. The increased signal that is obtained through the RDFM ionization scheme will allow for the study of coated particles [18,3]. These types of particles are important in the effort to distinguish uptake that occurs due to surface versus bulk reaction between a particle and gas phase species such as ozone or OH radicals. Additionally, real atmospheric particles are more likely to be mixtures of different compounds. Therefore, the use of an ionization method with a photon energy much closer to the ionization potential of most organic species than the 118 nm photon previously used will give less fragmentation. This will enhance the ability to study compounds in complex mixtures. The current set-up is limited to a single wavelength of 142 nm because only a single dye laser is used to generate the 212 nm precursor and the 425 nm difference frequency. With a second dye laser the 425 nm light currently used to down shift the output photon, can be made variable so that variable energy VUV light in this region can be generated. This would allow the VUV light energy to be tuned close to the ionization energy of specific compounds in the mixture so that they may be studied individually. On the other hand, the additional complexity of a tunable source would prohibit its use as a portable instrument in the field. The ideal approach for multi-component analysis is clearly MS/MS and an attempt at such an approach has been tried [36].

3.4. The use of rare gas resonance lamps

Although the RDFM method is extremely effective in a laboratory environment, the size of the set-up and the delicate aspects of laser alignment prevent it from being used in portable field instruments. An attractive alternative is the use of rare gas resonance lamps [37]. Kr (10.0 eV) and Xe (8.4 eV) lamps can be produced in a compact format (Syagen Inc.) and should provide up to 10^{15} photons per second. If these photons can be effectively directed into the ionization region, such lamps should produce the same signal as pulsed lasers. A flux of 10 particles per second with a 1 μm diameter (or 10^4 particles per second with a diameter of 100 nm) would produce a mass flow of 4.2×10^{-12} g/s assuming a particle density of 0.80 g/cm^3. Because the gas flow into the aerodynamic lens of our instrument is about 1 cm^3/s, such a mass flux would be generated by an atmospheric particle density of 4.2 μg/m^3, which is a reasonable density for clean atmospheres (typical urban atmospheres have a density of ∼20–100 μg/m^3) [17]. If the particles are vaporized and generate oleic acid molecules with a mean velocity of 2×10^4 cm/s, and the gas is returned in a 1 cm^2 cross-sectional area, the average gas density in the ionization region will be 4.5×10^5 oleic acid molecules/cm^3. Given a photoionization cross-section of 10^{-18} cm^2 and a photon flux of 10^{15} photons/s, the expected signal level is about 500 ions per second.

There is a major difference in the predicted ion signals of the continuous and pulsed light sources. For a large particle flow (1 μm diameter) of 10 particles per second, the pulsed laser with its 10^{10} photons per pulse can be efficiently used because it is fired only when a substantial gas density is generated by the arrival of a large particle. We expect that the peak gas density will be higher by a factor of 3000 thereby generating ions at the rate of 150 ions per second, even though the photon flux is only 10^{10} photons per pulse. This estimate is actually lower than our experimental signal, perhaps a result of our conservative estimation of the ionization cross-section.

These calculations show that the signal levels for a flow of 1 μm particles is about the same for the pulsed laser operating with 10^{10} photons per pulse and the continuous source with 10^{15} photons per second. However, if the particles are small, the pulsed laser loses its efficiency and its low photon flux prevents its use. The continuous source of 10^{15} photons per second, on the other hand, is equally efficient (or inefficient) for particles of any size and depends only on the total mass flux, and not on its temporal distribution.

4. Conclusion

The comparison between the 8.75 eV photons generated by resonance difference four-wave mixing (RDFM) and the 10.48 eV photons generated by third harmonic generation (THG) demonstrates that the lower energy pulsed laser photons are much more effective in giving fragmentation free spectra of organic constituents of aerosol particles. The test was carried out with oleic acid, a molecule of interest in atmospheric chemistry. The reduced ion fragmentation also results in a stronger parent peak signal. The results indicate that infrared CO_2 laser vaporization, especially at high IR laser pulse energies, produces vapor with a non-uniform temperature distribution as evidenced by mass spectra that depend upon the IR/VUV laser delay time. We suggest that this is a result of either non-uniform heating of the aerosol particle by the CO_2 laser, or of particle cooling as the outer layers of the particle vaporize. Using a heater for the vaporization step provides a more homogeneous temperature profile within the particles. In both cases, the dissociation of oleic acid is shown to be slow on the timescale of the experiment, which suggests that fragmentation free mass spectra are more likely if the ions are quickly extracted from the ionization region. Work is currently being done on the experiment to spatially separate λ = 142 and 212 nm to prevent any 1 + 1 REMPI from occurring, which should further decrease the intensity of the $m/z = 264$ water loss peak. Finally, we show that a continuous lamp with a photon flux of about 10^{15} photons per second should be an ideal ionization source for the detection of organic species in large and small aerosol particles.

Acknowledgements

We thank the National Science Foundation and the Air Force Office of Scientific Research (AFOSR) for financial

support. We also thank Profs. John Hepburn and Myung Soo Kim for help in setting up the resonance frequency difference mixing scheme.

References

[1] M.V. Johnston, A.S. Wexler, Anal. Chem. 67 (1995) 721A.
[2] K.R. Neubauer, M.V. Johnston, A.S. Wexler, Int. J. Mass Spectrom. Ion Processes 163 (1997) 29.
[3] E. Woods III, G.D. Smith, R.E. Miller, T. Baer, Anal. Chem. 74 (2002) 1642.
[4] E. Woods III, G.D. Smith, Y. Dessiaterik, T. Baer, R.E. Miller, Anal. Chem. 73 (2001) 2317.
[5] P.T.A. Reilly, A.C. Lazar, R.A. Gieray, W.B. Whitten, J.M. Ramsey, Aerosol Sci. Technol. 33 (2000) 135.
[6] M. Yang, P.T.A. Reilly, K.B. Boraas, W.B. Whitten, J.M. Ramsey, Rapid Commun. Mass Spectrom. 10 (1996) 347.
[7] K.A. Prather, T. Nordmeyer, K. Salt, Anal. Chem. 66 (1994) 1403.
[8] Z. Ge, A.S. Wexler, M.V. Johnston, Environ. Sci. Technol. 32 (1998) 3218.
[9] A.M. Middlebrook, D.M. Murphy, S.-H. Lee, D.S. Thompson, K.A. Prather, R.J. Wenzel, D.-Y. Liu, D.J. Phares, K.P. Rhoads, A.S. Wexler, M.V. Johnston, J.L. Jimenez, J.T. Jayne, D.R. Worsnop, I. Yourshaw, J.H. Seinfeld, R.C. Flagan, J. Geophys. Res. 108 (2003) SOS 12/1.
[10] D.S. Gross, M.E. Galli, P.J. Silva, S.H. Wood, D.Y. Liu, K.A. Prather, Aerosol Sci. Technol. 32 (2000) 152.
[11] L.S. Hughes, J.O. Allen, P. Bhave, M.J. Kleeman, G.R. Cass, D.Y. Liu, D.P. Fergenson, B.D. Morrical, K.A. Prather, Environ. Sci. Technol. 34 (2000) 3058.
[12] M.R. Alfara, H. Coe, J.D. Allan, K.N. Bower, H. Boudries, M.R. Canagaratna, J.L. Jimenez, J.T. Jayne, A.A. Garforth, S.M. Li, D.R. Worsnop, Atmos. Environ. 38 (2004) 5745.
[13] Q. Zhang, C.O. Stanier, M.R. Canagaratna, J.T. Jayne, D.R. Worsnop, S.N. Pandis, J.L. Jimenez, Environ. Sci. Technol. 38 (2004) 4797.
[14] M.R. Canagaratna, J.T. Jayne, D.A. Ghertner, S. Scott, Q. Shi, J.L. Jimenez, P.J. Silva, P. Williams, T. Lanni, F. Drewnik, K.L. Demerjian, C.E. Kolb, D.R. Worsnop, Aerosol Sci. Technol. 38 (2004) 555.
[15] D.J. Cziczo, D.M. Murphy, P.K. Hudson, D.S. Thomson, J. Geophys. Res. 109 (2004) D04201.
[16] D.J. Cziczo, D.M. Murphy, D.S. Thomson, M.N. Ross, Geophys. Res. Lett. 29 (2002) 33/1.
[17] B.J. Finlayson-Pitts, J.N. Pitts, Chemistry of the upper and lower atmosphere: theory, experiments and applications, Academic Press, New York, 2000.
[18] Y. Katrib, S.T. Martin, H.M. Hung, Y. Rudich, H. Zhang, J.G. Slowik, P. Davidovits, J.T. Jayne, D.R. Worsnop, JCPA 108 (2004) 6686.
[19] J.T. Jayne, D.C. Leard, X. Zhang, P. Davidovits, K.A. Smith, C.E. Kolb, D.R. Worsnop, Aerosol Sci. Technol. 33 (2000) 49.
[20] J.D. Hearn, G.D. Smith, Anal. Chem. 76 (2004) 2820.
[21] J.D. Hearn, G.D. Smith, J. Phys. Chem. A 108 (2004) 10019.
[22] P.J. Silva, K.A. Prather, Anal. Chem. 72 (2000) 3553.
[23] K. Salt, C.A. Noble, K.A. Prather, Anal. Chem. 68 (1996) 230.
[24] B. Oektem, M.P. Tolocka, M.V. Johnston, Anal. Chem. 76 (2004) 253.
[25] G.D. Smith, E. Woods III, C. Hauser, R.E. Miller, T. Baer, J. Phys. Chem. A 106 (2002) 8085.
[26] A. Amirav, J. Phys. Chem. 94 (1990) 5200.
[27] A. Amirav, A. Danon, Int. J. Mass Spectrom. Ion Processes 97 (1990) 107.
[28] B.W. LaFranchi, G.A. Petrucci, J. Am. Soc. Mass Spectrom. 15 (2004) 424.
[29] B.W. LaFranchi, J. Zahardis, G.A. Petrucci, Rapid Commun. Mass Spectrom. 18 (2004) 2517.
[30] P. Liu, P.J. Ziemann, D.B. Kittelson, P.H. McMurry, Aerosol Sci. Technol. 22 (1995) 293.
[31] P. Liu, P.J. Ziemann, D.B. Kittelson, P.H. McMurry, Aerosol Sci. Technol. 22 (1995) 314.
[32] J.W. Hepburn, in: A.B. Myers, T.R. Rizzo (Eds.), Laser Techniques in Chemistry, John Wiley and Sons Inc., New York, 1995, p. 149.
[33] T. Baer, J.A. Booze, K.M. Weitzel, in: C.Y. Ng (Ed.), Vacuum Ultraviolet Photoionization and Photodissociation of molecules and clusters, World Scientific, Singapore, 1991, p. 259.
[34] B. Sztáray, T. Baer, Rev. Sci. Instrum. 74 (2003) 3763.
[35] C. Sykes, E. Woods III, G.D. Smith, T. Baer, R.E. Miller, Anal. Chem. 73 (2001) 2048.
[36] R.A. Gieray, P.T.A. Reilly, M. Yang, M.B. Whitten, J.M. Ramsey, Anal. Chem. 70 (1998) 117.
[37] J.A.R. Samson, Techniques of Vacuum Ultraviolet Spectroscopy, Wiley, New York, 1967.